NEURAL REGENERATION RESEARCH
www.nrronline.org

Research Article

Osteopontin is a biomarker for early autoimmune uveoretinitis

https://doi.org/10.4103/1673-5374.330614
Date of submission: April 30, 2021
Date of decision: June 11, 2021
Date of acceptance: July 12, 2021
Date of web publication: December 10, 2021

Jeongtae Kim[1], Meejung Ahn[2], Yuna Choi[3], Jiyoon Chun[3], Kyungsook Jung[4], Akane Tanaka[5], Hiroshi Matsuda[5], Taekyun Shin[3, *]

From the Contents

Graphical Abstract *Upregulation of osteopontin (OPN) has adverse effects on inflammatory response and protective effects on experimental autoimmune uveoretinitis*

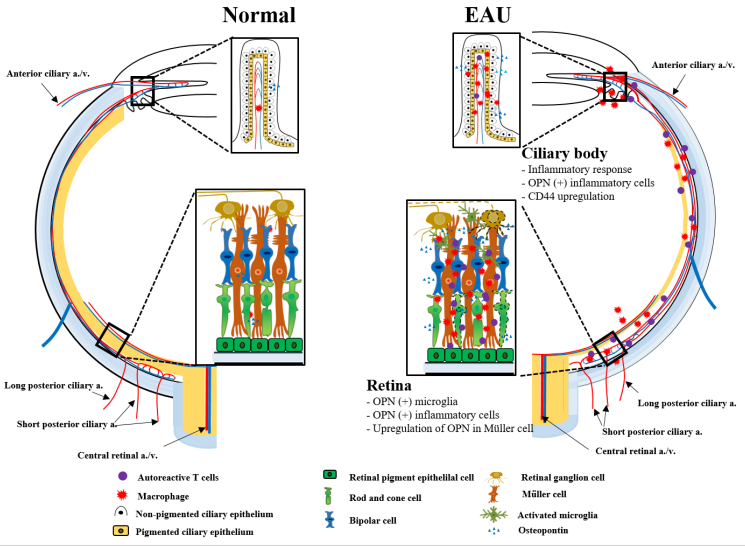

Abstract

Osteopontin (OPN) is an extracellular matrix protein with a diverse range of functions, including roles in cell adhesion, migration, and immunomodulation, which are associated with the modulation of neuroinflammation in the central nervous system. The present study was performed to evaluate the involvement of OPN in the eyes of an experimental autoimmune uveoretinitis (EAU) model. The EAU model was developed by immunization of Lewis rats with interphotoreceptor retinoid-binding protein. The results showed the OPN level was remarkably upregulated in the eye of EAU rats on day 9 post-immunization. The level of CD44, a ligand of OPN, was increased in the ciliary body of EAU rats. Furthermore, OPN was also detected in the ciliary body and activated microglia/macrophages in the EAU retina. The results suggest that OPN was significantly upregulated in the eyes of EAU rats, and that it may be useful as an early biomarker of ocular autoimmune diseases. All animal experiments were approved by the Institutional Animal Care and Use Committee of Jeju National University (approval No. 2020-0012) on March 11, 2020.

Key Words: CD44; ciliary body; experimental autoimmune uveoretinitis; macrophage; Müller cell; osteopontin; photoreceptor cell; retina

Chinese Library Classification No. R446; R364; R774

Introduction

Experimental autoimmune uveoretinitis (EAU) is a model of human autoimmune uveitis, which is characterized by autoimmune T lymphocyte infiltration into the uvea in susceptible animals (Diedrichs-Mohring et al., 2018; Huang et al., 2018). During the EAU process, peripherally generated T cells enter the circulation followed by infiltration of inflammatory cells into the uvea, including the iris and ciliary body, via adhesion to vascular endothelial cells (Diedrichs-Mohring et al., 2018). Once inflammatory cells have infiltrated the choroid and anterior chamber, inflammatory cells and their secretory mediators influence adjacent tissues, including the retina via the retinal pigment epithelium as well as the cornea across the anterior chamber (Pepple et al., 2016). The retina in EAU is influenced either by direct infiltration of inflammatory cells across the blood-retina barrier (Diedrichs-Mohring et al., 2018) or by indirect effects on the activated

[1]Department of Anatomy, Kosin University College of Medicine, Busan, Republic of Korea; [2]Department of Animal Science, College of Life Science, Sangji University, Wonju, Republic of Korea; [3]Department of Veterinary Anatomy, College of Veterinary Medicine and Veterinary Medical Research Institute, Jeju National University, Jeju, Republic of Korea; [4]Functional Biomaterials Research Center, Korea Research Institute of Bioscience and Biotechnology, Jeonbuk, Republic of Korea; [5]Laboratory of Comparative Animal Medicine, Division of Animal Life Science, Institute of Agriculture, Tokyo University of Agriculture and Technology, Tokyo, Japan

***Correspondence to:** Taekyun Shin, DVM, PhD, shint@jejunu.ac.kr.
https://orcid.org/0000-0002-9851-4354 (Taekyun Shin)

Funding: *This study was supported by the National Research Foundation of Korea, No. NRF-2019R1A2C1087753 (to TS).*
How to cite this article: *Kim J, Ahn M, Choi Y, Chun J, Jung K, Tanaka A, Matsuda H, Shin T (2022) Osteopontin is a biomarker for early autoimmune uveoretinitis. Neural Regen Res 17(7):1604-1608.*

retinal pigment epithelium, leading to detachment of photoreceptor cells from the retinal pigment epithelium (Benhar et al., 2016). This results in retinal degeneration, leading to visual dysfunction coincident with the activation of glia by oxidative stress (Saraswathy and Rao, 2008). In the pathogenesis of EAU, extracellular matrix proteins, including osteopontin (OPN), are involved in the initiation of inflammation and/or regeneration of injured tissues.

OPN, also known as secreted phosphoprotein 1, has a variety of biological activities, including cell adhesion, migration, survival, and activation of immune cells (Giachelli and Steitz, 2000; Denhardt et al., 2001), and these activities are partly mediated by the binding of OPN to cluster of differentiation (CD) 44 as an OPN ligand (Icer and Gezmen-Karadag, 2018). In addition, OPN is involved in neuro-inflammation, possibly mediating cell migration into nervous tissues (Shin, 2012). OPN plays an important role in the initiation of inflammation in autoimmune disease models, including experimental autoimmune encephalomyelitis, experimental autoimmune neuritis and experimental autoimmune myocarditis (Shin, 2012). Furthermore, OPN has been known as an early biomarker in rat cerebral cortex with cryolesion (Shin, 2012), and spinal cords with clip compression injury (Shin, 2012).

In the eye, OPN is constitutively expressed in retinal ganglion cells (RGCs) (Duan et al., 2015), Müller cells (Ruzafa et al., 2018) and retinal pigment epithelium (Hollborn et al., 2020). Functionally, OPN is involved in tissue regeneration in the cornea (Fujita et al., 2010) and survival of RGCs against ischemic injury (Chidlow et al., 2008). Although OPN is associated with homeostasis of the eye under normal conditions, the roles of OPN in the pathogenesis of autoimmune eye diseases remain to be elucidated.

EAU is a distinct ocular disease involving infiltration of autoimmune T cells and bystander cells into the uvea as well as the retina (Diedrichs-Mohring et al., 2018). Regarding ocular inflammation in EAU, which is characterized by infiltration of inflammatory cells (Diedrichs-Mohring et al., 2018), it is possible that OPN in the eye (including the cornea and retina) changes dynamically during the pathogenesis of EAU, particularly during the early stages of the disease. This study was performed to determine the localization of OPN in the EAU eye to understand its role in the course of autoimmune ocular disease.

Materials and Methods

Animals

Both male and female Lewis rats (6–8 weeks old, total number = 15; Orient Bio Inc., Gyeonggi-do, Republic of Korea) were housed in our animal facility under laboratory conditions (12-hour light/dark cycle, temperature 24 ± 2°C, convey system) and fed a standard diet (SAFE+40RMM; SAFE DIETS, Rosenberg, Germany). Experimental animals were randomly divided into three groups: normal control (*n* = 5), adjuvant control (*n* = 5), and EAU-induced rats (*n* = 5), and were maintained 5 rats per cage with JRS 3–4s bedding (SAFE, Rosenberg, Germany). All experimental procedures were performed in accordance with the Guidelines for the Institutional Animal Care and Use Committee of Jeju National University (approval No. 2020-0012) on March 11, 2020. All animal protocols conformed to international laws and National Institutes of Health (NIH) policies, including the Care and Use of Laboratory Animals (NIH publication No. 85-23, 1985, revised 1996). Every effort was made to reduce the number of animals and minimize their suffering.

Induction of EAU

The immunogens were emulsified in an equal volume (1 mg/mL) of bovine interphotoreceptor retinoid-binding protein (peptide sequence: PTARSVGAADGSSWEGVGVVPDV; Koma Biotech, Seoul, Republic of Korea) and complete Freund's adjuvant (CFA) supplemented with 1 mg/mL Mycobacterium tuberculosis H37Ra (Difco Laboratories Inc., Detroit, MI, USA). Lewis rats (*n* = 5) were immunized by injection of 100 µL of the emulsion into each hindlimb footpad. As an adjuvant control (*n* = 5), an equal volume of CFA was inoculated into the hindlimb footpads of rats. Age-matched normal rats (*n* = 5) without immunization were used as normal controls. Sampling date was selected based on the previous study (Diedrichs-Mohring et al., 2018).

Tissue sampling

To investigate the change of OPN in the early stage of EAU, eye tissues were sampled on day 9 post-immunization based on the previous study (Diedrichs-Mohring et al., 2018). The experimental rats were sacrificed under deep anesthesia via CO_2 gas inhalation (95% CO_2, acryl chamber: 25 cm × 40 cm × 26 cm) on day 9 post-immunization. After euthanasia, both eyes were collected (one for western blot analysis and one for immunostaining.), fixed in 4% paraformaldehyde in phosphate buffered saline (PBS), and processed for embedding in paraffin. Eye tissue sections were cut into 5-µm-thick sections using a microtome (RM 2135; Leica, Nussloch, Germany) and stained with hematoxylin and eosin for histopathological examination. Eye tissue sections were deparaffinzed with xylene (I, II, and III) and in a graded ethyl alcohol solution (100%, 95%, 90%, 80%, and 70%), and reacted with hematoxylin solution (Easy stain Harris Hematoxylin, YD Diagnostics CORP., Gyeonggi-do, Republic of Korea) for 5 minutes. Then, sections were washed with tap water for 5 minutes and reacted with eosin solution (Clear ViewTM Eosin, BBC Biochemical, McKinney, TX, USA) for 30 seconds. After dehydration with a graded ethyl alcohol solution (90%, 95% and 100%), sections were cleared with xylene and mounted with HistomountTM (national diagnostic, Atlanta, USA). Furthermore, the collected eye tissues for western blot analysis were stored in the deep freezer (–80°C) until use.

Antibodies used in this study

The antibodies used in this study are summarized in **Table 1**.

Western blot analysis

Western blot analysis was performed as described previously (Kim et al., 2020). Briefly, the retina (*n* = 3 per group) was homogenized in lysis buffer containing protease and phosphatase inhibitors. Samples were subjected to electrophoresis and then transferred onto nitrocellulose membranes (Schleicher and Schuell, Keene, NH, USA). The membranes were blocked with 10% skim milk (v/v) in Tris-buffered saline (TBS), then reacted with primary antibodies against mouse anti-OPN (1:1000; sc-21742, Santa Cruz Biotechnology, Santa Cruz, CA, USA) and β-actin (1:10,000; A5441, Sigma-Aldrich, St. Louis, MO, USA) (**Table 1**) overnight at 4°C. After washing three times with TBS, the nitrocellulose membranes were incubated with secondary antibody such as mouse immunoglobulin G (IgG) (1:1000; Vector Laboratories, PI-2000, Burlingame, CA, USA) and reacted with BS ECL Plus Kit reagent (W6002; Biosesang, Gyeonggi-do, Republic of Korea). Positive signals were captured and analyzed by Fusion Solo 6X software (Vilber Lourmat, Collégien, France). OPN expression level was normalized to that of β-actin.

Table 1 | **Characterization of antibodies**

Antigen	Immunogen	Manufacturer, species and antibody type	Dilution
CD44	Rat T blasts from mixed lymphocyte reactions (OX-49)	BD PharmingenTM (Cat# 554869, Lot. 0000042442), mouse, monoclonal	1:200
Iba1	Recombinant full length protein of human	Abcam (Cat# ab15690, Lot. LKH4161), mouse, monoclonal	1:1000
GS	Purified GS from sheep brain	Chemicon International (MAB302), mouse, monoclonal	1:10,000
β-Actin	Synthetic β-cytoplasmic actin N-terminal peptide conjugated to KLH	Sigma-Aldrich (Cat# a5441, Lot. 028K4826), mouse, monoclonal	1:10,000
OPN	Recombinant OPN of mouse OPN origin	Santa Cruz Biotechnology, Inc. (Cat# sc-21742, Lot. AKm2A1), mouse, monoclonal	1:1000
OPN	Synthetic peptide corresponding to human OPN aa 170–183	Abcam (Cat# ab8448, Lot. GR3286062-13), rabbit, polyclonal	1:400
Secondary antibodies for immunohistochemistry			
Biotinylated goat anti-rabbit IgG		Vector Laboratories (PK-6101, VECTASTAIN Elite ABC Rabbit IgG Kit)	1:200
Biotinylated horse anti-mouse IgG		Vector Laboratories (PK-6102, VECTASTAIN Elite ABC Mouse IgG Kit)	1:200
Secondary antibodies for western blot analysis			
Peroxidase anti-mouse IgG (H + L)		Vector Laboratories (Cat# PI-2000, Lot. ZC1212)	1:1000

aa: Amino acids; GS: glutamine synthetase; Iba1: ionized calcium binding adaptor molecule 1; IgG: immunoglobulin G; OPN: osteopontin.

Immunohistochemical and immunofluorescence staining

Immunohistochemistry was performed to localize the antigens using the Vectastain Elite ABC Kit (Vector Laboratories, Burlingame, CA, USA) as described previously (Kim et al., 2020). Briefly, deparaffinized eye tissue sections were blocked with normal goat serum, followed by incubation with rabbit anti-OPN (1:400; ab8448, Abcam, London, UK) for 2 hours and then the corresponding biotinylated goat anti-rabbit IgG at room temperature. After washing with PBS, horseradish peroxidase-labeled avidin was applied to the sections using the Elite ABC Kit (Vector Laboratories). The peroxidase reaction was performed using a peroxidase substrate kit (DAB, SK-4100; Vector Laboratories), and the reaction was stopped using distilled water. Sections were counterstained with hematoxylin to visualize the target signals. Three different researchers independently observed.

Double-labeling immunofluorescence was performed to localize antigens in specific cell types. Briefly, the deparaffinized sections were treated with 10% normal goat serum for 1 hour and then with the first primary antibody (i.e., rabbit anti-OPN; ab8448, Abcam) overnight at 4°C, and subsequently reacted with corresponding biotinylated secondary antibody (goat anti-rabbit IgG). The slides were then reacted with tetramethyl rhodamine isothiocyanate-conjugated streptavidin (1:500, 016-020-084, Lot. 117099; Jackson ImmunoResearch Laboratories, Inc., West Grove, PA, USA) for 1 hour at room temperature. Next, the sections were washed and incubated with the second primary antibody, i.e., mouse anti-ionized calcium binding adaptor molecule 1 (Iba1; ab115690, Abcam) or mouse anti-glutamine synthetase (Chemicon International, Temecula, CA, USA), overnight at 4°C. After washing, the sections were incubated with corresponding biotinylated horse anti-mouse IgG and reacted with fluorescein isothiocyanate-conjugated streptavidin (1:500, 43-4311, Lot. 50594970; Zymed Laboratories Inc., San Francisco, CA, USA) for 1 hour at room temperature. Next, the slides were examined under a fluorescence microscope (BX-51; Olympus, Tokyo, Japan) and photographed, and the images were merged using Adobe Photoshop 7.0 software (Adobe Systems, San Jose, CA, USA).

Statistical analysis

We calculated the sample size of this experiment based on the previous studies (Charan and Kantharia, 2013; Diedrichs-Mohring et al., 2018; Choi et al., 2021). Furthermore, the number of experimental animals in the present study is 5 per group. Based on the sample size calculating formula (Charan and Kantharia, 2013), the sample size was revealed to be an appropriate size. No animals were excluded from the analysis. Two different researchers performed the western blot assay and immunohistochemistry, independently. All values are presented as the mean ± standard error of the mean (SEM) of three independent experiments. The results were analyzed using one-way analysis of variance followed by the Student-Newman-Keuls *post hoc* test for multiple comparisons using the GraphPad Prism Version 7 software (GraphPad Software Inc., San Diego, CA, USA). In all analyses, $P < 0.05$ was taken to indicate statistical significance.

Results

Ocular inflammation

Under microscopic observation, the presence of round cells was confirmed in the ciliary body (**Figure 1C**) and retina (**Figure 1F**) of EAU rats, whereas these cells were not observed in normal controls (**Figure 1A** and **D**) or rats administered CFA only (**Figure 1B** and **E**). Numerous round cells (inflammatory cells) were detected in the anterior and posterior chambers near the ciliary body (**Figure 1C**). Furthermore, retinal detachment was confirmed in some EAU rats (data not shown).

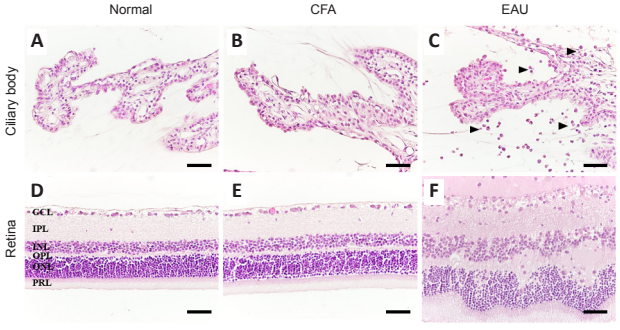

Figure 1 | **Histopathological changes in the retina of normal control, complete Freund's adjuvant (CFA)-only, and experimental autoimmune uveoretinitis (EAU) rats.**
There were no inflammatory cells in the ciliary body of the normal control (A) and CFA-only (B) groups. However, inflammatory cells (arrowheads) were detected in the ciliary body of EAU rats (C). The cytoarchitecture of the retina was well organized in normal control and CFA-only rats (D and E). On the other hand, disruption of the retinal structure and retinal inflammation were observed in the EAU rats (F). Scale bars: 40 μm. GCL: Ganglion cell layer; INL: inner nucleus layer; IPL: inner plexiform layer; ONL: outer nucleus layer; OPN: outer plexiform layer; PRL: photoreceptor layer.

OPN upregulation in the eye of EAU rats

Western blot analysis confirmed the upregulation of OPN in the EAU rats compared with normal control and CFA-only rats (**Figure 2**). The levels of both the OPN precursor (predicted size 66 kDa) and OPN cleavage product (predicted size 25–55 kDa) were increased in the ocular tissue of EAU rats compared with normal control and CFA-only rats (**Figure 2A**), with significant increases in the retina (both $P < 0.05$) (**Figure 2B**).

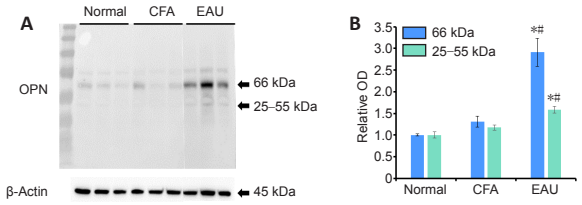

Figure 2 | Western blot analysis of osteopontin (OPN) in the retina of normal control, CFA-only, and EAU rats.
(A) Western blot analysis of OPN (approximately 66 kDa) and its cleavage product (approximately 25–55 kDa) was performed. The protein level of OPN was increased in the retina of EAU rats compared with normal control and CFA-only rats. Furthermore, the band of 25–55 kDa, corresponding to the OPN cleavage product, was detected in the EAU rats. (B) The bar graphs show quantification of OPN expression relative to β-actin expression. **P* < 0.05, *vs.* normal control rats, #*P* < 0.05, *vs.* CFA-only rats (one-way analysis of variance followed by the Student-Newman-Keuls *post hoc* test). Bar graphs are the mean ± standard error of the mean (SEM) of three independent experiments (*n* = 3).

Next, we determined the OPN expression pattern in the eye. OPN immunoreactivity was detected in the ciliary body in the normal control and CFA-only groups (**Figure 3A** and **B**) and was markedly increased in the round cells around the ciliary body in EAU rats (**Figure 3C**). CD44, which interacts with OPN, was also upregulated in the ciliary body of EAU rats (**Figure 3F**) compared with the normal control and CFA-only groups (**Figure 3D** and **E**). Furthermore, OPN was localized in the RGC layer, inner plexiform layer, inner nucleus layer, and outer plexiform layer in the normal control and CFA-only groups (**Figure 4A** and **B**). The intensity of OPN immunoreactivity was increased in all layers of the retina in EAU rats (**Figure 4C**).

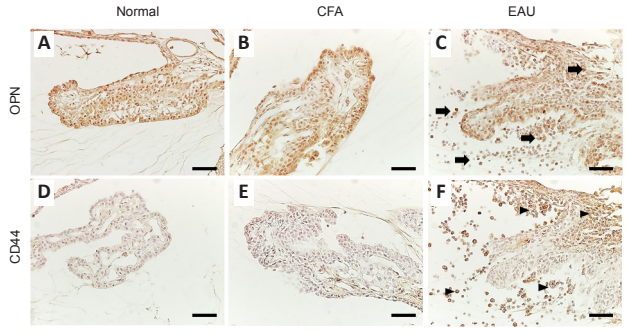

Figure 3 | Immunohistochemical staining of OPN and CD44 in the ciliary body of normal control, CFA-only, and EAU rats.
Compared with the normal control (A) and CFA-only groups (B), OPN immunoreactivity was increased in the EAU rats (arrows, C). The immunoreactivity of CD44, a ligand of OPN, was weak in the normal control (D) and CFA-only rats (E). CD44 immunoreactivity was strong in EAU rats (arrowheads, F). Both OPN and CD44 were strongly detected in the inflammatory cells of EAU rats (C, F). Arrows: OPN-positive cells; arrowheads: CD44-positive cells. Scale bars: 40 μm. CFA: complete Freund's adjuvant; EAU: experimental autoimmune uveoretinitis; OPN: outer plexiform layer.

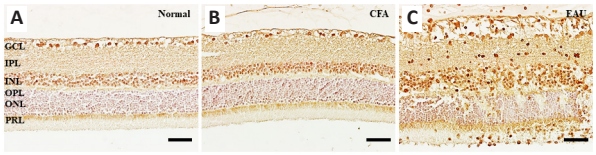

Figure 4 | Immunohistochemical staining of OPN in the retina of the normal control, CFA-only, and EAU rats.
OPN immunoreactivity was detected in the ganglion cell layer, inner plexiform layer, inner nucleus layer, and outer plexiform layer of the retina in the normal control group (A) and CFA-only group (B). However, the intensity of OPN staining was elevated in the retina of EAU rats (C). Scale bars: 40 μm. GCL: Ganglion cell layer; INL: inner nucleus layer; IPL: inner plexiform layer; ONL: outer nucleus layer; OPN: outer plexiform layer; PRL: photoreceptor layer.

Phenotype of OPN-expressing cells

To investigate the phenotype of OPN-expressing cells in the ciliary body and retina, we performed double fluorescence staining in the eyes of normal control and EAU rats. OPN immunoreactivity was colocalized with Iba1-positive inflammatory cells in the ciliary body of EAU rats (**Figure 5D**), but not in normal control rats (**Figure 5A**). Furthermore, OPN was detected strongly in Iba1-positive microglia (**Figure 5E**) and glutamine synthetase-positive Müller cells in the retina (**Figure 5F**), compared with those of normal control rats (**Figure 5B** and **C**, respectively).

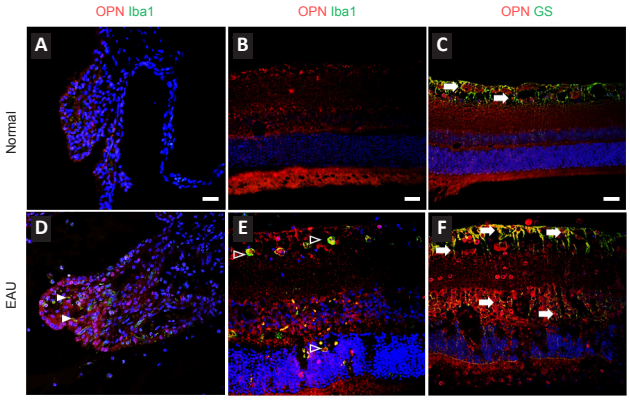

Figure 5 | Double immunofluorescence staining of OPN and ionized calcium binding adaptor molecule 1 (Iba1) or glutamine synthetase (GS) in the ciliary body and retina of normal control and EAU rats.
OPN was colocalized with Iba1-positive inflammatory cells in the ciliary body (arrowheads in D) and Iba1-positive microglia in the retina (hallow arrowheads in E), but not in normal control (A and B, respectively). Furthermore, OPN was strongly detected in GS-positive Müller cells (arrows in F), compared with that of normal control (arrows in C). Scale bars: 40 μm.

Discussion

This is the first confirmation that constitutive OPN is upregulated in the eyes, including the ciliary body and retina, of EAU rats. Increased levels of both the OPN precursor and OPN cleavage product were detected in inflammatory and glial cells, such as microglia and Müller cells, during the induction stage of EAU. These results suggested that OPN facilitates inflammation in rats during the early stages of EAU.

In the retina, OPN expression was reported in the RGCs of normal rats and in activated microglia/macrophages and $CD4^+$ T cells in EAU (Hikita et al., 2006; Chidlow et al., 2008) and rat glaucoma (Yu et al., 2021), suggesting that OPN is a pro-inflammatory mediator in the EAU model. These findings further support the observation that OPN-knockout mice showed reduced clinical symptoms, including less lymphocyte proliferation and infiltration after induction of EAU by immunization with the interphotoreceptor retinoid-binding protein (Hikita et al., 2006). Furthermore, OPN was detected in vitreal cells and the epiretinal membrane in patients subjected to therapeutic vitreoretinal surgery (Dinice et al., 2020). In addition, induction of OPN via inhibition of CD47 signaling caused by high-temperature requirement A serine peptidase 1 has a pro-inflammatory effect in models of subretinal inflammation and age-related macular degeneration (Beguier et al., 2020). Therefore, we postulated that upregulation of OPN in microglia/macrophages of the ciliary body and retina is strongly associated with the induction of uveoretinitis during the early stages of EAU.

OPN is elevated in both inactive and active fibrovascular membranes in proliferative diabetic retinopathy and is activated by Wnt/β-catenin effector lymphoid enhancing binding factor 1 (LEF1) (Gong et al., 2018). In human autoimmune disease, T cell proliferation is suppressed by

Wnt/β-catenin in the Wnt signaling pathway via promotion of transcription factors, including T cell factor 1 and LEF1 (Wildner and Kaufmann, 2013). Blocking of OPN by small interfering RNA mitigates T cell proliferation and suppresses the increased levels of inflammatory cytokines in EAU mice (Iwata et al., 2010). Furthermore, inflammatory T cells and macrophages are the main sources of OPN in the spinal cord and sciatic nerve in experimental autoimmune neuritis in animals (Shin, 2012). Therefore, we postulate that upregulation of OPN in T cells promotes inflammatory responses in the uvea and retina of EAU rats.

OPN has been shown to play a dual role in neuroinflammation, with both neuroinflammatory and neuroprotective effects (Shin, 2012). In retinal Müller cells, OPN has been shown to be associated with the enhancement of survival of primary RGCs *in vitro* (Ruzafa et al., 2018), a decreased OPN level was closely associated with a reduced neuroprotective effect in the retina during extracellular matrix remodeling in equine recurrent uveitis with downregulation of fibronectin, an extracellular matrix glycoprotein, in Müller cells (Deeg et al., 2011). Furthermore, OPN from Müller cells has neuroprotective effects in the primary porcine photoreceptor cells and the retinal explants of the retinal degeneration 1 mutant mice (Del Rio et al., 2011). Regarding other sources of OPN in the eye, OPN produced by retinal pigment epithelial cells, which is induced by the cellular danger signal ATP, promotes photoreceptor survival via basic fibroblast growth factor in cultured retinal pigment epithelial cells (Hollborn et al., 2020). Therefore, our results suggest that an increased OPN level in Müller cells contributes to the survival of photoreceptor cells and RGCs in the retina of EAU rats during the early stages.

There are limitations in this study. We have focused on the tissue level of OPN in the eyes with EAU as well as the cellular localization. However, the evaluation of OPN in the sera of rats with EAU was not performed to further verify whether OPN was a good indicator in the course of EAU.

Taken together, these observations suggest that OPN and CD44 are constitutively localized in the inflammatory cells, microglia, and Müller cells of the eye and upregulated after immunization in EAU as in other autoimmune diseases. The transient upregulation of OPN in macrophages and microglia during the induction stage of EAU suggested that OPN may be involved in inflammatory responses. On the other hand, upregulation of OPN in Müller cells may have a protective effect on photoreceptor cells and RGCs. Therefore, OPN is recommended as an early biomarker of EAU. However, the precise mechanisms need further exploration.

Author contributions: *Study concept and manuscript review: JK, MA, YC, JC, AT, HM, TS; study design: TS; definition of intellectual content: AT, HM, TS; literature retrieval: KJ, MA, YC, TS; implementation of experimental studies: KJ, MA, YC, JC, TS; data acquisition: JK, MA, YC, JC, TS; data analysis: JK, YC, JC, TS; statistical analysis: KJ, MA, TS; manuscript preparation and editing: KJ, TS; guarantor: TS. All authors approved the final version of this paper.*
Conflicts of interest: *All authors declared that they have no conflicts of interest.*
Financial support: *This study was supported by the National Research Foundation of Korea, No. NRF-2019R1A2C1087753 (to TS).*
Institutional review board statement: *All experimental procedures were performed in accordance with the Guidelines for the Care and Use of Laboratory Animals of Jeju National University (approval No. 2020-0012) on March 11, 2020.*

Data sharing statement: *Datasets analyzed during the current study are available from the corresponding author on reasonable request.*
Plagiarism check: *Checked twice by iThenticate.*
Peer review: *Externally peer reviewed.*

References

Beguier F, Housset M, Roubeix C, Augustin S, Zagar Y, Nous C, Mathis T, Eandi C, Benchaboune M, Drame-Maigné A, Carpentier W, Chardonnet S, Touhami S, Blot G, Conart JB, Charles-Messance H, Potey A, Girmens JF, Paques M, Blond F, et al. (2020) The 10q26 risk haplotype of age-related macular degeneration aggravates subretinal inflammation by impairing monocyte elimination. Immunity 53:429-441.e8.
Benhar I, Reemst K, Kalchenko V, Schwartz M (2016) The retinal pigment epithelium as a gateway for monocyte trafficking into the eye. EMBO J 35:1219-1235.
Charan J, Kantharia ND (2013) How to calculate sample size in animal studies. J Pharmacol Pharmacother 4:303-306.
Chidlow G, Wood JP, Manavis J, Osborne NN, Casson RJ (2008) Expression of osteopontin in the rat retina: effects of excitotoxic and ischemic injuries. Invest Ophthalmol Vis Sci 49:762-771.
Choi Y, Jung K, Kim H, Chun J, Ahn M, Jee Y, Ko H, Moon, Matsuda H, Tanaka A, Kim J, Shin T (2021) Attenuation of experimental autoimmune uveitis in Lewis rats by betaine. Exp Neurobiol 30:308-317.
Deeg CA, Eberhardt C, Hofmaier F, Amann B, Hauck SM (2011) Osteopontin and fibronectin levels are decreased in vitreous of autoimmune uveitis and retinal expression of both proteins indicates ECM re-modeling. PLoS One 6:e27674-27674.
Del Rio P, Irmler M, Arango-Gonzalez B, Favor J, Bobe C, Bartsch U, Vecino E, Beckers J, Hauck SM, Ueffing M (2011) GDNF-induced osteopontin from Muller glial cells promotes photoreceptor survival in the Pde6brd1 mouse model of retinal degeneration. Glia 59:821-832.
Denhardt DT, Noda M, O'Regan AW, Pavlin D, Berman JS (2001) Osteopontin as a means to cope with environmental insults: regulation of inflammation, tissue remodeling, and cell survival. J Clin Invest 107:1055-1061.
Diedrichs-Mohring M, Kaufmann U, Wildner G (2018) The immunopathogenesis of chronic and relapsing autoimmune uveitis-Lessons from experimental rat models. Prog Retin Eye Res 65:107-126.
Dinice L, Cacciamani A, Esposito G, Taurone S, Carletti R, Ripandelli G, Artico M, Micera A (2020) Osteopontin in vitreous and idiopathic epiretinal membranes. Graefes Arch Clin Exp Ophthalmol 258:1503-1513.
Duan X, Qiao M, Bei F, Kim IJ, He Z, Sanes JR (2015) Subtype-specific regeneration of retinal ganglion cells following axotomy: effects of osteopontin and mTOR signaling. Neuron 85:1244-1256.
Fujita N, Fujita S, Okada Y, Fujita K, Kitano A, Yamanaka O, Miyamoto T, Kon S, Uede T, Rittling SR, Denhardt DT, Saika S (2010) Impaired angiogenic response in the corneas of mice lacking osteopontin. Invest Ophthalmol Vis Sci 51:790-794.
Giachelli CM, Steitz S (2000) Osteopontin: a versatile regulator of inflammation and biomineralization. Matrix Biol 19:615-622.
Gong MT, Li WX, Zhang Q, Lv WW, He ZH, Zhou SL, Zhang H, Wang J, He K (2018) Comprehensive analysis of gene expression profiles associated with proliferative diabetic retinopathy. Exp Ther Med 16:3539-3545.
Hikita ST, Vistica BP, Jones HR, Keswani JR, Watson MM, Ericson VR, Ayoub GS, Gery I, Clegg DO (2006) Osteopontin is proinflammatory in experimental autoimmune uveitis. Investigative ophthalmology & visual science 47:4435-4443.
Hollborn M, Bruck R, Kuhrt H, Wiedemann P, Bringmann A (2020) Osmotic and hypoxic induction of osteopontin in retinal pigment epithelial cells: Involvement of purinergic receptor signaling. Mol Vis 26:188-203.
Huang XT, Wang B, Zhang WH, Peng MQ, Lin D (2018) Total glucosides of paeony suppresses experimental autoimmune uveitis in association with inhibition of Th1 and Th2 cell function in mice. Int J Immunopathol Pharmacol 32:394632017751547.
Icer MA, Gezmen-Karadag M (2018) The multiple functions and mechanisms of osteopontin. Clin Biochem 59:17-24.
Iwata D, Kitamura M, Kitaichi N, Saito Y, Kon S, Namba K, Morimoto J, Ebihara A, Kitamei H, Yoshida K, Ishida S, Ohno S, Uede T, Onoe K, Iwabuchi K (2010) Prevention of experimental autoimmune uveoretinitis by blockade of osteopontin with small interfering RNA. Exp Eye Res 90:41-48.
Kim J, Ahn M, Choi Y, Shin T (2020) Upregulation of cathepsins in olfactory bulbs is associated with transient olfactory dysfunction in mice with experimental autoimmune encephalomyelitis. Mol Neurobiol 57:3412-3423.
Pepple KL, Choi WJ, Wilson L, Van Gelder RN, Wang RK (2016) Quantitative assessment of anterior segment inflammation in a rat model of uveitis using spectral-domain optical coherence tomography. Invest Ophthalmol Vis Sci 57:3567-3575.
Ruzafa N, Pereiro X, Lepper MF, Hauck SM, Vecino E (2018) A proteomics approach to identify candidate proteins secreted by muller glia that protect ganglion cells in the retina. Proteomics 18:e1700321.
Saraswathy S, Rao NA (2008) Photoreceptor mitochondrial oxidative stress in experimental autoimmune uveitis. Ophthalmic Res 40:160-164.
Shin T (2012) Osteopontin as a two-sided mediator in acute neuroinflammation in rat models. Acta Histochem 114:749-754.
Wildner G, Kaufmann U (2013) What causes relapses of autoimmune diseases? The etiological role of autoreactive T cells. Autoimmun Rev 12:1070-1075.
Yu H, Zhong H, Li N, Chen K, Chen J, Sun J, Xu L, Wang J, Zhang M, Liu X, Deng L, Huang P, Huang S, Shen X, Zhong Y (2021) Osteopontin activates retinal microglia causing retinal ganglion cells loss via p38 MAPK signaling pathway in glaucoma. FASEB J 35:e21405.

C-Editor: Zhao M; S-Editor: Li CH; L-Editor: Song LP; T-Editor: Jia Y